Photochemistry and Photobiology, 2004, 80: 242–249

Bioluminescence Imaging of the Response of Rat Gliosarcoma to ALA-PpIX–mediated Photodynamic Therapy¶

Eduardo H. Moriyama[1,2], Stuart K. Bisland[1], Lothar Lilge[1] and Brian C. Wilson*[1]

[1]Department of Medical Biophysics, Ontario Cancer Institute, University of Toronto, Toronto, Ontario, Canada
[2]Instituto de Pesquisa e Desenvolvimento, Universidade do Vale do Paraíba, São José dos Campos, SP, Brazil

Received 18 February 2004; accepted 15 June 2004

ABSTRACT

Photodynamic therapy (PDT) is a promising modality for the treatment of solid tumors that combines a photosensitizing agent and light to produce cytotoxic reactive oxygen species that lead to tumor cell death. The recent introduction of bioluminescence imaging (BLI), involving the use of the luciferase gene (*luc*) transferred into target tumor cells, followed by systemic administration of luciferin and detection of the emitted visible chemiluminescence photons, offers the potential for longitudinal imaging of tumor growth and therapeutic response in single animals. We demonstrate in this study the first results of the use of BLI to assess the response of an intracranial brain tumor model (9L rat gliosarcoma) to aminolevulinic acid (ALA)–mediated PDT. Complementary *in vitro* experiments with the luciferase-transfected 9L cells show that the decrease in the luminescent signal after PDT correlates with cell kill. *In vivo* imaging shows a decrease in the BLI signal from the tumor after ALA-PDT treatment, followed by tumor regrowth. Furthermore, preliminary studies using cells transfected with a hypoxia-responsive vector show an increase in bioluminescence within 4 h after Photofrin-mediated PDT, demonstrating the ability to observe stress-gene responses. These results suggest that BLI can be used to provide spatiotemporal information of intracranial brain tumor responses after PDT and may serve as a valuable response-endpoint measure.

INTRODUCTION

Photodynamic therapy (PDT) is an evolving treatment modality for neoplastic and nonneoplastic diseases (1). It is based on the accumulation of a photosensitizing drug into target cells or tissues, followed by activation using light of an appropriate wavelength to generate cytotoxic intermediates, such as singlet oxygen ($^1O_2$), resulting in direct cell death via necrosis or apoptosis (2) or indirect tumor cell death induced by tumor ischemia due to vascular damage (2,3), depending on the photosensitizer, tissue and treatment parameters.

We have a specific interest in the use of PDT to treat malignant brain tumors and we (4–6) and others (7–9) have shown in preclinical studies that PDT mediated by the hematoporphyrin derivative photosensitizer Photofrin® (Axcan Pharma., Quebec, Canada) can cause tumor destruction. In addition, we (5) and others (10) have shown similar results in Phase I–II clinical trials, in which PDT is given as an adjuvant to surgical resection, potentially resulting in improved survival or increased time to recurrence in this invariably fatal disease. However, as demonstrated in a rodent model bearing intracranially implanted tumors, PDT mediated by Photofrin and several other photosensitizers can cause significant damage to normal brain tissue in addition to inducing necrosis in tumor (4). The exception to this has been protoporphyrin IX (PpIX) induced endogenously by the administration of the prodrug 5-aminolevulinic acid (ALA), which increases heme biosynthesis in cells. ALA-PpIX–mediated PDT appears to be highly selective for tumor *versus* normal brain (especially white matter) (4,11). Recently, we have also shown (12) in 9L rat gliosarcoma tumor grown intracranially that PDT with low doses of ALA or light can induce tumor cell–specific apoptosis with no significant damage to normal brain cells. However, the fraction of tumor cells killed per ''dose'' is small, so repeated treatments or continuous drug and light administration for an extended period will be required to achieve tumor control. This approach, termed metronomic (12,13) to distinguish it from standard (acute) PDT treatment using a single high dose of photosensitizer and light, will require new treatment-monitoring tools, preferably including longitudinal studies in single animals.

Monitoring the tumor response during PDT treatments, either acute or metronomic, is critical in evaluating new photosensitizers, in determining dose–response relationships and in assessing the effect of treatment modifiers (14). *In vivo*, it is particularly important to have a method to follow tumor growth and response in individual animals in order to reduce the subject-to-subject variability and, hence, the number of animals required for statistical analysis. For intracranial tumors, a further motivation is that induction involves complex surgical procedures, so that the number of tumor-bearing animals that can be generated is limited. Several different response-monitoring techniques have been reported, including magnetic resonance imaging (MRI) or spectroscopy (15), X-ray computed tomography (CT) imaging

¶Posted on the website on 23 June 2004.

*To whom correspondence should be addressed: Department of Medical Biophysics, Ontario Cancer Institute, University of Toronto, 610 University Avenue, Room 7-417, Toronto, Ontario, Canada M5G 2M9. Fax: 416-946-6529; e-mail: wilson@uhnres.utoronto.ca

Abbreviations: ALA, aminolevulinic acid; ATP, adenosine triphosphate; BLI, bioluminescence imaging; CCD, charge-coupled device; CT, computed tomography; FBS, fetal bovine serum; HIF-1, hypoxia-inducible factor 1; $9L^{luc}$, luciferase-transfected 9L; MRI, magnetic resonance imaging; mTHPC, *meso*-tetrahydroxyphenyl chlorin; PBS, phosphate-buffered saline; PDT, photodynamic therapy; PpIX, protoporphyrin IX; SRB, sulforhodamine-B.

© 2004 American Society for Photobiology 0031-8655/04 $5.00+0.00

(16), (Doppler) ultrasound imaging (17), positron emission tomography (18) and electrical impedance spectroscopy (19,20). Optical methods investigated or proposed to date include laser Doppler imaging (21), photoacoustic imaging (22) and (Doppler) optical coherence tomography (23,24). Fluorescence spectroscopy–imaging of photosensitizer photobleaching has also been evaluated (25), as has spectroscopic measurement of photoproducts generated during treatment (26). These various techniques report different structural or functional (or both) characteristics of the tumor tissue in response to treatment, and each has its own strengths and limitations. None is yet established as a ''routine'' method, either in preclinical or clinical studies.

In this study, we report on the use of bioluminescence imaging (BLI) for monitoring the brain tumor response to PDT. BLI has been developed over the past few years (27,28) and, in its most common implementation, involves transfection of the firefly luciferase (*luc*) gene, in this case into the tumor cells. Upon administration of the substrate luciferin (D-(–)-2(6′-hydroxy-2′-benzothiazolyl)thiazone-4-carboxylic acid) and in the presence of adenosine triphosphate (ATP) and oxygen, luciferase catalyzes the conversion of luciferin into oxyluciferin, accompanied by the emission of light in the 400–620 nm range, with a maximum at around 562 nm. The sequence of reactions is given below.

$$\text{Luciferase} + \text{Luciferin} + \text{ATP} + \text{Mg} \Leftrightarrow \text{Luciferase} \cdot \text{Luciferin} - \text{AMP} + \text{Ppi}, \quad (1a)$$

$$\text{Luciferase} \cdot \text{Luciferin} - \text{AMP} + \text{O}_2 \rightarrow \text{Luciferase} \cdot \text{Oxyluciferin}^+ + \text{AMP} + \text{CO}_2, \quad (1b)$$

$$\text{Luciferase} \cdot \text{Oxyluciferin}^+ \rightarrow \text{Luciferase} \cdot \text{Oxyluciferin} + \text{Light}, \quad (1c)$$

where AMP is adenosine monophosphate and Ppi is pyrophosphate.

Bioluminescence measurements can be done in nonimaging mode (luminometry), and we have used this method in this study to assess the ALA-PDT response of brain tumor cells *in vitro*. With transfected cells grown as solid tumors *in vivo,* the bioluminescence light is emitted shortly after systemic administration of luciferin. A fraction of the emitted light is transmitted through the tissues overlying the tumor and, with the animal in a light-tight box to reduce background ambient light, can be detected externally by a sensitive charge-coupled device (CCD) camera. The general advantages of BLI are that it has very low-level background and does not require an excitation light source and that there should be a linear relationship between the light signal and the number of light-emitting cells (29–31). Importantly for therapeutic response monitoring, BLI detects only live, metabolically active tumor cells, whereas other imaging techniques such as CT or MRI do not distinguish between live and dead or nonfunctioning cells (30,32). Tumor growth and treatment responses can be followed longitudinally in single animals by repeated administration of luciferin because this has low toxicity and clears rapidly from tissues.

There have been a number of studies of BLI for monitoring tumor responses to different treatments (29,33–35). Of particular interest, Rehemtulla *et al*. (33) reported the use of sequential BLI monitoring of the response of intracranial luciferase-transfected 9L ($9L^{luc}$) tumors to chemotherapy with 1,3-bis(2-chloroethyl)-1-nitrosourea. MRI was done at the same time, from which the tumor volume was measured from the contrast-enhancing regions. For BLI, the total number of bioluminescence photons within the region of interest in the brain was counted for a fixed time (1 min) after intraperitoneal injection of luciferin at 150 mg/kg body weight. The two measures showed very similar time curves, both before and after drug treatment, and the authors highlighted the advantages of BLI in observing only metabolically active cells after tumor treatment.

There have been only a few reports of bioluminescence explicitly for monitoring PDT responses. Schlosser *et al*. (36) used luminometry to measure the responses of four different ovarian cancer cell lines *in vitro* after *meso*-tetrahydroxyphenyl chlorin (mTHPC)–mediated PDT. The intracellular ATP level was measured as a way to assess cell viability after PDT, and a good correlation between the bioluminescence signal and the number of viable cells was observed. More recently, Hamblin *et al*. (37,38) investigated bacteria strains transfected with the bacterial luciferase (*lux*) gene that were used to infect skin wounds in mice. PDT was performed using a polycationic photosensitizer conjugate (poly-L-lysine-C_{e6}), and BLI demonstrated quantitatively bacterial killing as a function of PDT dose and time after treatment.

This study comprises, first, the use of luminometry to confirm the correlation between the bioluminescence signal and PDT-induced brain tumor cell kill *in vitro* and, second, the evaluation of BLI for longitudinal monitoring of intracranial tumor response *in vivo* following PDT.

MATERIALS AND METHODS

Cell transfection. The tumor model used both *in vitro* and *in vivo* was the rat 9L gliosarcoma (39). The cells were grown as monolayers in Dulbecco's medium (GIBCO BRL, Ontario, Canada) supplemented with 10% fetal bovine serum (FBS), penicillin (100 μg/mL) and streptomycin (100 μg/mL) in 5% CO_2 at 37°C in a humidified incubator. The modified firefly luciferase gene plasmid (pGL3 enhancer vector: Promega, Madison, WI) was cotransfected into 9L cells with a vector containing a neomycin selection marker (pCI mammalian expression vector: Promega) at a ratio of 10:1. For the primary selection, the $9L^{luc}$ cells were grown with Dulbecco's medium containing 700 μg/mL of antibiotic G418 sulfate (Promega) for 10 days. The antibiotic-resistant colonies were isolated, and a second selection was performed to identify and isolate the transfectants with the highest luciferase expression. For this, 5×10^3 cells were seeded per well into 96-well plates, and after adding 100 μL of luciferin (D-luciferin potassium salt: Promega) solution (1 m*M* in phosphate-buffered saline, PBS), the bioluminescence signal was counted for a 60 s integration period in an automatic luminometer (LB96V: Berthold, Oak Ridge, TN). The cell line used for all subsequent studies was that with the highest light emission among the 14 luminescence-positive colonies found (~four-fold higher than the next highest colony). The resulting $9L^{luc}$ cells were cultured as monolayers in air-filtered 175 cm^2 Nunclon flasks (Fisher Scientific, Ontario, Canada) under the same conditions as above, except for a reduced concentration of antibiotic G418 sulfate (350 μg/mL).

Intracellular PpIX measurements. In the use of bioluminescence for studying PDT responses, it is important that the photocytotoxicity of the transfected cells is comparable with that of the parental cell line. The concentration and microdistribution of the intracellular photosensitizer is a key determinant of photocytotoxicity in PDT. Hence, as the first step we compared the levels of ALA-induced PpIX between 9L and $9L^{luc}$ cells. This is particularly important because PpIX synthesis in the mitochondria is itself an ATP-dependent process (40). For each experiment, 2×10^3 cells were grown in the dark on coverslips incubated for 0 (control), 1, 2 or 4 h in serum-free media containing 1 m*M* of ALA (Frontier Scientific Corp., Logan, UT) without pH buffer. The coverslips were then rinsed once with PBS, and the cells were examined under a confocal microscope (LSM510: Zeiss, Jena, Germany) using an excitation wavelength of 543 nm and detecting the fluorescence above 600 nm. For semiquantitative evaluation of intracellular PpIX concentration, the fluorescence intensity was integrated within defined extranuclear regions of interest.

In vitro *PDT treatment and response assays.* To determine the changes in cellular bioluminescence after PDT treatment *in vitro*, monolayers of $9L^{luc}$ cells were incubated in 96-well plates (5×10^3 cells/well) with 1 m*M* of serum-free ALA in media for 4 h. The ALA-containing media was then

removed and replaced by fresh, ALA-free media containing 10% FBS. Cells were exposed to 30 J/cm^2 of 635 nm light from a diode laser (Photonics Research Ontario, Ontario, Canada) expanded to a uniform-intensity, 4 cm diameter beam to illuminate groups of 3 × 3 wells simultaneously at 14 mW/cm^2. First, cell viability was assessed 24 and 48 h after PDT by adding 100 μL of luciferin solution (1 m*M* in PBS) and counting the bioluminescence photons for a 60 s integration period in an automatic luminometer (LB96V: Berthold). Second, cell viability was confirmed using the sulforhodamine-B (SRB) colorimetric assay. In brief, after luminometric measurements, cells were fixed with 100 μL of 10% trichloroacetic acid (Sigma Aldrich Corp., Oakville, ON, Canada) per well and kept at 4°C for 1 h, followed by staining with 50 μL of 4% SRB for 30 min at room temperature. Unbound SRB was removed by washing with 1% acetic acid, and the preparation was air-dried overnight. The resulting precipitate was dissolved in 100 μL unbuffered 10 m*M* Tris solution at pH 10.5 (Sigma Aldrich Corp.). The optical density was determined by an automated spectrophotometric plate reader (MCC/340: MTX Labs, Vienna, VA) at 540 nm, using 690 nm subtraction for background absorbance.

To compare the PDT responses of the parental 9L and the 9L^{luc} cells, a colony-forming assay was performed. In brief, preconfluent 9L and 9L^{luc} cells were harvested using trypsin, plated in 3.5 cm petri dishes at 1000 cells/dish and allowed to adhere overnight. These were then washed once with PBS, and the media were replaced with 5 mL of serum-free media containing 1 m*M* ALA. After 4 h, the drug-containing media were removed and the dishes washed once with PBS and replaced with complete fresh growth media. Plates were irradiated on a light box ($\lambda > 600$ nm) at 14 mW/cm^2, which does not induce any significant temperature rise. After the start of light irradiation, individual samples were removed when they had received their predetermined radiant exposure level (10, 20 or 30 J/cm^2). The control group for each cell line did not receive drug or light. Immediately after irradiation, cells were harvested using trypsin, plated in 100 mm petri dishes with full media and returned to the incubator for 7 days. Resulting colonies were stained with methylene blue, and colonies containing >20 cells were counted. Both the 9L and 9L^{luc} cells were treated using the same procedures to minimize possible bias.

In vivo *tumor induction.* The *in vivo* PDT response was investigated using 9L^{luc} cells grown as intracranial solid tumors. All experiments were approved by the Animal Care Committee of University Health Network, Toronto, Canada. For tumor induction, 10 female Fischer rats (Charles River, Ontario, Canada) weighing 150–200 g were anesthetized by intraperitoneal injection of ketamine (80 mg/kg) and xylazine (13 mg/kg), and the head was immobilized in a stereotaxic frame. A 15 mm long incision was made along the midline of the skull, and the skin was reflected. Using a high-speed drill, a 2 mm burr hole was made in the left hemisphere, anterior to the coronal fissure. 9L^{luc} cells (5×10^3 in 5 μL of media) were injected into the caudal dienchephalon, 1.5 mm beneath the dura mater using a 26G Hamilton syringe, over a period of 5 min to avoid mechanical or pressure damage. The needle was slowly retracted, the burr hole left open and the skin sutured closed. Saline solution (3 mL) was administrated subcutaneously to prevent dehydration. This procedure led to formation of tumors of 2–3 mm diameter after 7–10 days of growth.

In vivo *BLI.* Bioluminescence images were collected 48 and 96 h after tumor implantation, at 72, 24 and 7 h before PDT light exposure (or sham treatment) and subsequently at 24, 48 and 72 h after treatment. For this, a commercial BLI system was used (IVIS System: Xenogen, Alameda, CA), comprising a cryogenically cooled, high-sensitivity CCD camera in a light-tight box. Commercial software (LivingImage™: Xenogen) was used to collect and analyze the images. For each imaging procedure, the rats were preanesthetized with 5% halothane–air mixture. A solution of luciferin (D-luciferin potassium salt: Promega) at a concentration of 40 mg/mL in saline was injected intraperitoneally at a dose of 40 mg/kg at 10 min before the start of imaging. The rat was then placed in the imaging chamber 20 cm below the imaging optics, allowing the whole animal to be imaged with a single field of view. During image acquisition, a 2% halothane–air mixture was delivered through a nose cone, and the body temperature was maintained at 37°C using a heated stage. A white-light image was obtained first to provide an anatomical reference for the bioluminescence image, which was then acquired with a 5 min integration time. A false-color image of the BLI photon counts was overlaid on the white-light image, and the total BLI counts from a region of interest over the cranium, including the tumor, were determined.

PDT treatments. In vivo PDT was performed once the tumors had grown large enough to give a BLI signal of ~5 × 10^7 counts. ALA in hydrochloride form was dissolved in physiologic saline (20 mg/mL) with the pH adjusted to 6.4–6.7 by 1 *N* NaOH and injected intravenously via the tail vein at a dose of 50 mg/kg at 6 h before light exposure. Light irradiation to the brain surface overlying the tumor was applied through the existing burr hole after turning the skin flap. A 635 nm diode laser was coupled to a 200 μm core optical fiber with a distal lens collimator to produce a uniform, 7 mm diameter beam over the burr hole. The exposure time was 470 s at an irradiance of approx. 50 mW/cm^2, resulting in 20 J/cm^2 radiant exposure. We have shown previously that this combination of ALA and light dose does not produce significant necrosis or apoptosis in normal brain tissue but does result in marked apoptosis in tumor (12,41). After irradiation, the skin was resutured, 3 mL of saline was injected subcutaneously as previously noted and the animals were left to recover in the dark. For this initial study, seven rats received PDT treatment. In addition, in three 9L^{luc}-bearing control animals, the same surgical and BLI imaging procedures were performed but no ALA or light irradiation was delivered. This ensures that the BLI changes seen after treatment were attributable to the PDT and not to the second surgical intervention.

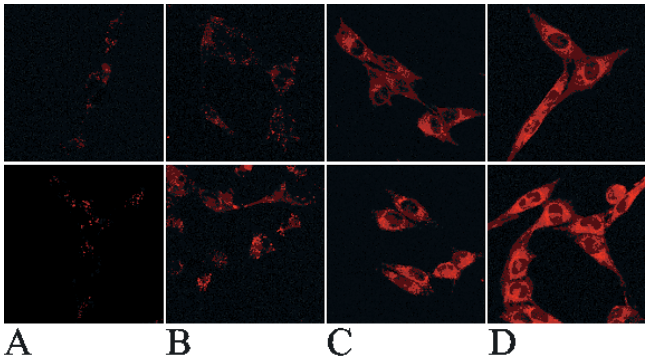

Figure 1. Confocal fluorescence images (λ_{ex} = 543 nm, λ_{em} > 600 nm) in 9L (upper) and 9L^{luc} (lower) cells. All images were obtained with the same microscope settings and imaging time. A: Control (no drug). B–D: 1, 2 and 4 h after incubation with 1 m*M* ALA in serum-free media.

RESULTS

Intracellular PpIX synthesis between parental and transfected cells

Figure 1 shows examples of confocal fluorescence images of 9L and 9L^{luc} cells *in vitro* for different ALA incubation times. The fluorescence increases with incubation time compared with the autofluorescence (control) background as the PpIX synthesis proceeds. Because PpIX synthesis takes place in the mitochondria (42), most of the PpIX fluorescence was observed within cytoplasmic and perinuclear areas, as expected. There are no marked qualitative differences in the pattern of fluorescence between 9L and 9L^{luc} cells. Figure 2 shows the relative cytoplasmatic PpIX concentrations, determined by measuring the intracellular fluorescence signal using Image J software, averaged over at least 10 randomly selected cells in each of three separate experiments. Regression analysis showed no statistically significant difference in PpIX levels between the 9L and 9L^{luc} cells (P = 0.001).

Bioluminescence as a means to measure cell viability

Figure 3 shows the good linearity between bioluminescence counts and different numbers of viable cells determined by a hemocytometer (Hausser Scientific, Horsham, PA) using the trypan blue dye exclusion assay. Figure 4 shows the change in cell survival, measured by the SRB assay, and in the corresponding bioluminescence signal in 9L^{luc} cells after ALA-PDT *in vitro*. Note

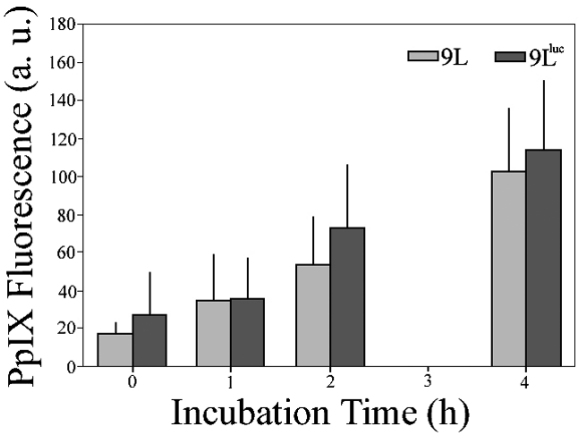

Figure 2. Intracellular PpIX (relative values) in 9L and $9L^{luc}$ cells *in vitro* as a function of incubation time with 1 m*M* ALA in serum-free media. Each value is the mean and standard deviation (mean ± SD) over three experiments, each comprising at least 10 cells.

that the SRB assay does not distinguish between necrotic and apoptotic cell death. Necrotic cell death is expected to cause complete loss of bioluminescence signal due to rapid ATP depletion caused by decline in mitochondria activity (43). In the case of apoptosis, since multiple pathways may be involved, we tested if the bioluminescence signal changed also with a purely apoptotic response, using 10 μg/mL cisplatin ($Cl_2H_6N_2Pt$, Fauldding, Quebec, Canada). The results are shown in Figure 5.

Comparison between PDT survival of the parental 9L and transfected $9L^{luc}$ cells, as shown in Fig. 6, suggests a slight but statistically significant reduction in sensitivity to radiance exposure at relatively low doses ($P < 0.005$ in the slope of the survival curve). Figure 2 indicates that this is probably not due to altered ALA uptake or PpIX synthesis. No statistically significant difference in percentage of cell survival was seen at higher ALA (2 m*M*) and light (60 J/cm^2) doses: 3.5 ± 0.47 for 9L and 4.0 ± 0.39 for $9L^{luc}$ ($P = 0.72$).

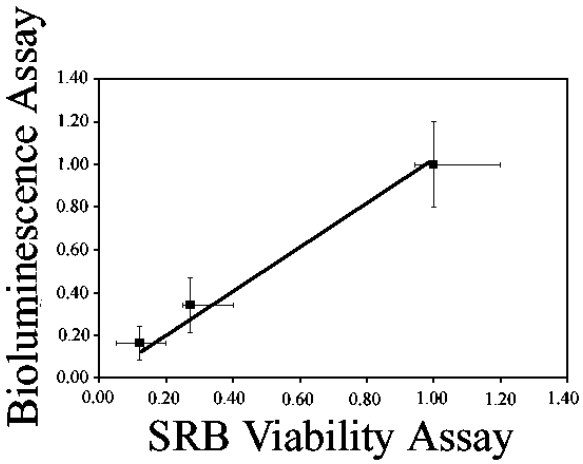

Figure 4. Correlation between colorimetric SRB viability assay and bioluminescence signal (mean ± SD for triplicate experiments) for $9L^{luc}$ cells *in vitro* after ALA-PDT (6 h incubation with 1 m*M* ALA, 14 J/cm^2 of 635 nm light). The fitted regression line is also shown ($r^2 = 0.984$).

In vivo changes in bioluminescence signal

Figure 7 shows an example of BLI *in vivo* in an individual intracranial $9L^{luc}$ tumor–bearing rat before and after PDT. We note that the brighter signal from the center of the tumor may be partly due to reduced attenuation of the light through the burr hole. The integrated bioluminescence signal from PDT-treated and control animals is shown in Fig. 8 averaged over all animals. A marked reduction in bioluminescence at 24 h post PDT was also seen in all treated animals individually (data not shown), suggesting a reduction of the number of viable tumor cells. The average log reduction in signal 24 h after treatment was 0.35 ± 0.2 (~50% reduction). By 48 h after treatment, tumor regrowth was observed. The pre- and post-treatment exponential growth rates were not significantly different: 0.57 ± 0.089 *versus* 0.56 ± 0.08, respectively.

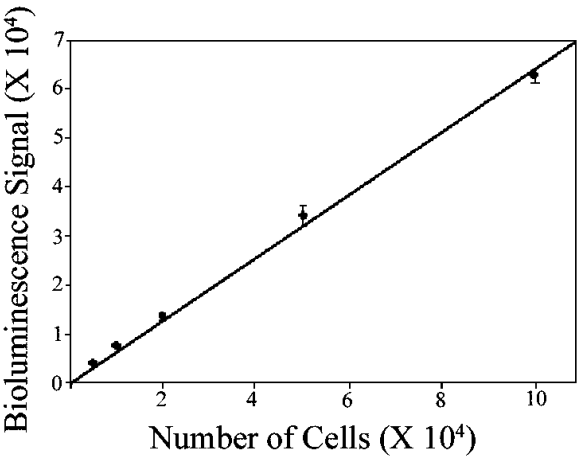

Figure 3. Bioluminescence signal (mean counts ± SD for triplicate experiments) *versus* the number of (untreated) $9L^{luc}$ cells in 96-well plates. The luminometer signal was integrated for 1 min immediately after adding 100 μL/well of 1 m*M* of D-luciferin solution. The line is the linear regression fit ($r^2 = 0.996$).

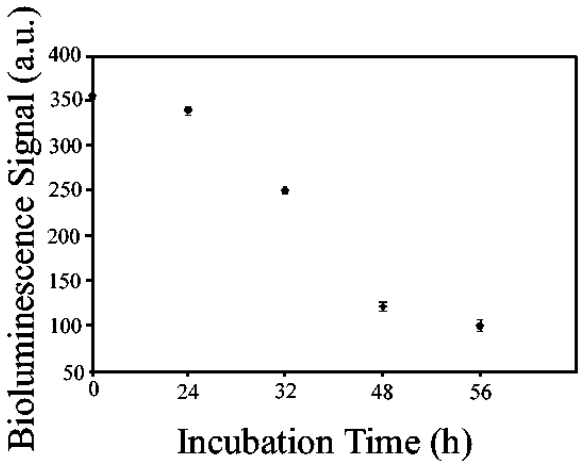

Figure 5. Bioluminescence response (mean ± SD for triplicate experiments) of $9L^{luc}$ cells *in vitro* to different incubation times in media containing cisplatin (10 μL/mL). Cells were seeded in 96-well plates at 5×10^3 cells/well at 24 h before treatment. The bioluminescence was measured as in Fig. 3.

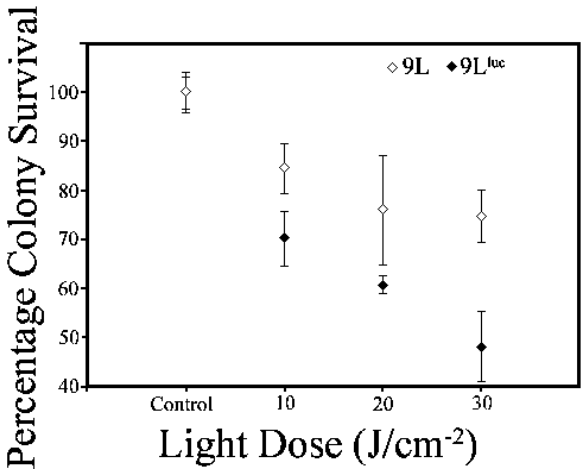

Figure 6. Comparison of PDT cell survival (colony-forming assay after PDT, 1 m*M* ALA for 4 h) as a function of irradiance between 9L and $9L^{luc}$ cells *in vitro*. The data for each cell line are normalized to their own no-treatment controls.

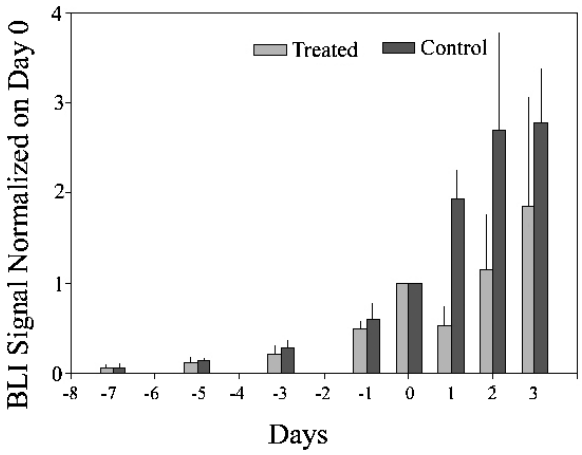

Figure 8. BLI counts (mean ± SD) during tumor growth, PDT response and post-treatment regrowth averaged over the seven treated animals or the three untreated controls, with the counts in each animal normalized to the value on Day 0.

DISCUSSION

The objective of this study was to evaluate the feasibility of using BLI on the response of intracranial tumors to PDT. The motivation is to use this technique in studies of PDT response under a range of different treatment conditions as part of ongoing development and optimization of acute- and metronomic-PDT for brain tumors (4,6,12,13,41). The potential benefit of this technique is the ability to track tumor growth, response and regrowth noninvasively over time in individual animals, complementing survival studies and measurements of tumor response made by histopathologic evaluation after sacrifice at specific time points. In addition, the observation of metabolically active tumor cells *in vivo* is of particular value in assessing apoptotic responses. There are, however, a number of potential limitations or artifacts that are intrinsic to the use of BLI as a quantitative tool to monitor PDT effects *in vivo*. These include (1) alteration of the photosensitizer concentration or PDT sensitivity due to luciferase gene transfection; (2) variations in BLI counts due to different depths of tumor in the brain, which alters the light attenuation; (3) variations in luciferin delivery to the tumor cells; and (4) possible changes in tumor oxygenation due to PDT-induced vascular responses that would alter the oxygen-dependent bioluminescence reaction.

Figures 1 and 2 show that Point (1) is probably not a significant concern in this study. Nevertheless, there may be some alteration in the PDT sensitivity (Fig. 6), so that it will be necessary to validate directly the *in vivo* BLI measurements with independent assays of tumor response, for example, using the terminal deoxynucleotidyl transferase–mediated deoxyuridine triphosphate nick end–labeling (TUNEL) assay for apoptosis, as we have used previously (12,41,44).

Our prior experience with the intracranial 9L model induced by careful, depth-controlled tumor cell injection into the brain (41) shows that the tumor depth and growth pattern are reasonably consistent between animals, so that the attenuation factor (Point 2) may be modest. However, this requires quantitative confirmation. Using the model studies of Rice *et al.* (30) on the tissue depth dependence of the BLI signal, we estimate that the difference in signal per viable cell between cells at the tumor surface and at 3 mm depth is <10% (using as the tissue optical properties, absorption coefficient $\mu_a = 0.5\ cm^{-1}$ and transport scattering coefficient $\mu_s' = 15\ cm^{-1}$). Hence, unless there is a marked asymmetry in tumor morphology with growth, which we have not seen in this model, differences in tumor depth should not significantly distort the BLI growth and response curves for individual animals but could cause variations between animals.

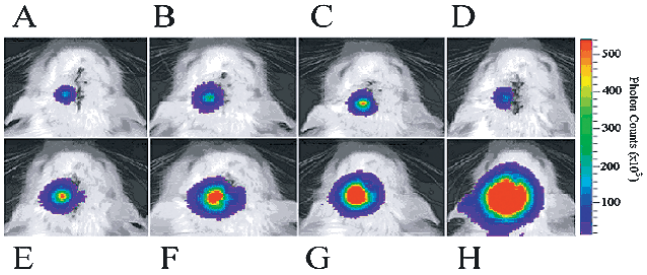

Figure 7. Example of successive *in vivo* bioluminescence images of intracranial $9L^{luc}$ tumor growth, PDT response and regrowth in the same animal. A–C: At 72, 24 and 6 h before PDT. D–H: At 24, 48 and 72 h and 7 and 10 days after PDT. Each image was collected for 5 min. The color scale bar indicates the photon count per pixel. PDT, 50 mg/kg ALA i.v., 20 J/cm^2 at 20 mW/cm^2 delivered 6 h after ALA.

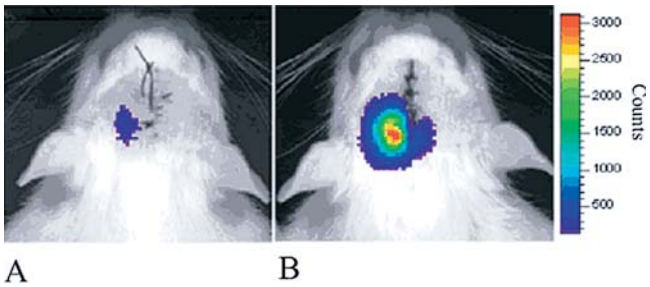

Figure 9. Example of altered gene expression induced by PDT. $9L^{HIF\text{-}1\text{-}luc}$ cells (5×10^3) were implanted 7 days before treatment. A: BLI image 2 h before Photofrin injection (12.5 mg/kg). PDT was performed 20 h later (40 J/cm^2) at 100 mW/cm^2 of 635 nm light. B: Four hours after PDT, showing a four-fold increase in luminescence in the tumor.

The growth rates before and after PDT should measure the true increases in viable tumor cell number, assuming that the depth attenuation effect is negligible. We note that Rehemtulla *et al.* (33) demonstrated good correlation between tumor volume and chemotherapeutic response measured by MRI and by BLI in the same 9L rat gliosarcoma model. This study also suggests that luciferin delivery is not a limiting factor in this model (Point 3), although these authors used a much higher concentration of luciferin with shorter measuring time, so that the experiments are not exactly comparable.

The data of Fig. 3 confirm the linearity of the bioluminescence signal with viable cell number so that, for example, the reduction in the BLI signal from the $9L^{luc}$ tumor *in vivo* immediately after PDT treatment should be proportional to the reduction in the number of viable cells due to treatment. However, we note an added complication with PDT is that, for surface light irradiation, the tumor response is strongly depth dependent: in previous studies of the density distribution of apoptotic bodies in brain, we found that the number of apoptotic cells is higher close to the treated tissue surface (41,44). The BLI signal then represents the integration of this depth response, weighted by the tissue attenuation effect, resulting in a bias toward the more superficial tumor cells. Interstitial fiber optic light delivery into the center of the tumor will be preferred in future studies to reduce this effect. The development of longer wavelength luciferases (45,46) would also make the measurements less sensitive to tissue attenuation and allow information from deeper tumor to be obtained.

For Point (4), ALA-PDT under the conditions used in this study predominantly produces a cellular response (41), so that we do not anticipate any substantial vascular changes. This will, however, become a substantive issue with higher PDT doses and, clearly, with vascularly-targeted photosensitizers such as Pd-bacteriopheophorbide that we are currently using for PDT of prostate cancer (47). Hence, we have initiated *in vitro* studies with controlled oxygen variation to quantify the oxygen dependence of the cellular bioluminescence signal.

According to Fig. 8, the average tumor growth rates before and after PDT are the same, although this was not true for all individual animals. Complications in comparing growth rates before and after treatment are that (1) there may be differences in the initial growth pattern, depending on the exact location of tumor cell injection; and (2) as stated above, surface PDT irradiation gives a strong light fluence-depth dependence, so that the depth distribution of the tumor cells also may have an important effect on the growth pattern after PDT.

In the experiments described above, we used cells that constitutively express the luciferase gene. This does not yield information about the mechanisms of cell death or the molecular pathways induced by PDT. The detection of early gene expression after treatment could help to identify the mechanisms of action underlying the response of tumor cells to PDT. The molecular responses induced by PDT have been investigated by several groups (48–50). In a first approach using reporter genes to identify the stress signaling induced by PDT, Mitra *et al.* (51) used the imaging of the green fluorescence protein reporter gene to analyze the activation of an HSP-70 promoter after mTHPC-PDT *in vivo*. Recently, Shibata *et al.* (52) have developed a hypoxia-inducible vector comprising five copies of hypoxia-responsive elements constructed with fragments of the human vascular endothelial growth factor gene (5HRE/hCMVmp-luc), where the transcription of the luciferase gene is regulated by the expression of the hypoxia-inducible factor 1 (HIF-1). We have used this vector in a preliminary test of the potential of BLI to observe *in vivo* changes in gene expression induced by PDT. For these experiments we used Photofrin®, rather than ALA-PpIX, because Photofrin-PDT is known to induce tumor cell death by vascular damage, resulting in tumor tissue hypoxia (2) and inducing the expression of HIF-1 transcriptional factor (53). Stable transfectants with this hypoxia-responsive vector were established using G418 selection (700 μg/mL) for 10 days. Cells were exposed to $CoCl_2$ (100 μ*M* for 24 h), which is known to mimic hypoxic conditions and to induce HIF-1 activation under normoxia (54). Positive luciferase cells were verified by addition of 0.5 m*M* of luciferin in PBS. The surgical procedures for tumor induction and PDT treatment were as described previously. Photofrin-PDT (12.5 mg/kg *i.v.* at 20 h before irradiation by 40 J/cm^2 of 635 nm laser light at 50 mW/cm^2) was given 7 days after tumor induction. Figure 9 shows that the bioluminescence signal is markedly increased (~four-fold above the baseline) within 4 h after treatment, demonstrating that BLI can be used as a noninvasive technique to study stress-gene expression after PDT (53).

Finally, we recently reported preliminary observations (55) that BLI has sufficient sensitivity to detect minimal residual $9L^{luc}$ cells *in situ* after ALA-PpIX fluorescence–guided surgical resection of intracranial tumor in the rat, even when there was no detectable residual PpIX fluorescence. Fluorescence-guided resection of malignant brain tumors is being developed by a number of groups (56,57), including ourselves (58), and we have proposed to use it before PDT in order to reduce the gross tumor burden by increasing the extent of resection (55). Hence, in preclinical studies, we anticipate being able to use BLI to track tumor growth before resection, minimal residual tumor postresection, PDT cytoreduction and tumor regrowth in individual animals. This should markedly accelerate the optimization of the combined treatment protocols.

Acknowledgements—This work was supported in part by the Canadian Cancer Society through a grant from the National Cancer Institute of Canada and by the U.S. National Institutes of Health (CA43892). The IVIS System was provided through a grant from the Canadian Foundation for Innovation. Technical developments were supported by the Canadian Institute for Photonic Innovations. E.H.M. was sponsored in part by Universidade do Vale do Paraíba, SP, Brazil. The authors thank Anoja Giles, Annie Lin, Lee Chin and Patrick Subarsky for technical assistance. The hypoxia-responsive transcription vector was kindly provided by Dr. Amato J. Giaccia, Stanford University, via Dr. Richard P. Hill, University Health Network, Toronto.

REFERENCES

1. Dougherty, T. J. (2002) An update on photodynamic therapy applications. *J. Clin. Laser Med. Surg.* **20**, 3–7.
2. Henderson, B. W. and T. J. Dougherty (1992) How does photodynamic therapy work? *Photochem. Photobiol.* **55**, 777–779.
3. Fingar, V. H., T. J. Wieman, S. A. Wiehle and P. B. Cerrito (1992) The role of microvascular damage in photodynamic therapy. The effect of treatment on vessel constriction, permeability, and leukocyte adhesion. *Cancer Res.* **52**, 4914–4921.
4. Lilge, L. and B. C. Wilson (1998) Photodynamic therapy of intracranial tissues: a preclinical comparative study of four different photosensitizers. *J. Clin. Laser Med. Surg.* **16**, 81–91.
5. Muller, P. J. and B. C. Wilson (1995) Photodynamic therapy for recurrent supratentorial gliomas. *Semin. Surg. Oncol.* **11**, 346–354.
6. Lilge, L., M. C. Olivo, S. W. Schatz, J. A. McGuire, M. S. Patterson and B. C. Wilson (1996) The sensitivity of normal brain and intracranial implanted VX2 tumour to interstitial photodynamic therapy. *Br. J. Cancer* **73**, 332–343.

7. Chopp, M., M. O. Dereski, V. Madigan, F. Jiang and B. Logie (1996) Sensitivity of 9L gliosarcomas to photodynamic therapy. *Radiat. Res.* **146**, 461–465.
8. Jiang, F., L. Lilge, J. Grenier, Y. Li, M. D. Wilson and M. Chopp (1997) Photodynamic therapy of U87 human glioma in nude rat using liposome-delivered Photofrin. *Lasers Surg. Med.* **22**, 74–78.
9. Jiang, F., L. Lilge, B. Logie, Y. Liand and M. Chopp (1997) Photodynamic therapy of 9L gliosarcoma with liposome-delivered Photofrin. *Photochem. Photobiol.* **65**, 701–706.
10. Kaye, A. H., G. Morstyn and D. Brownbill (1987) Adjuvant high-dose photoradiation therapy in the treatment of cerebral glioma: a phase 1–2 study. *J. Neurosurg.* **67**, 500–505.
11. Olivo, M. and B. C. Wilson (2004) Mapping ALA-PPIX fluorescence in normal brain and brain tumour using confocal fluorescence microscopy. *Int. J. Oncol.* **25**, 37–45.
12. Wilson, B. C., L. D. Lilge, S. K. Bisland, A. Bogaards and P. Muller (2003) Pre-clinical studies of metronomic photodynamic therapy (mPDT) using ALA-PpIX for selective apoptosis of intracranial malignant glioma. *Proc. SPIE* **4952**, 23–31.
13. Bisland, S. K., L. Lilge, A. Lin, R. Rusnov and B. C. Wilson (2004) Metronomic photodynamic therapy as a new paradigm for photodynamic therapy: rationale and preclinical evaluation of technical feasibility for treating malignant brain tumors. *Photochem. Photobiol.* **80**, 22–30.
14. Wilson, B. C., M. S. Patterson and L. Lilge (1997) Implicit and explicit dosimetry in photodynamic therapy, a new paradigm. *Lasers Med. Sci.* **12**, 182–199.
15. Powers, S. K., S. S. Cush, D. L. Walstad and L. Kwock (1991) Stereotactic intratumoral photodynamic therapy for recurrent malignant brain tumors. *Neurosurgery* **29**, 688–695.
16. Yeung, I., L. D. Lilge and B. C. Wilson (1997) Photodynamic therapy (PDT) induced alterations of the blood-brain-barrier transfer constant of a tracer molecule in normal brain. *Proc. SPIE* **2972**, 54–63.
17. Yang, V. X. D., G. J. Gzarnota, I. A. Vitkin, M. Kolios, M. Sherar, J. de Boer, B. Tromberg and B. C. Wilson (2002) Ultrasound backscatter microscopy/spectroscopy and optical coherence (Doppler) tomography for mechanism-specific monitoring of photodynamic therapy in vivo and in vitro. *Proc. SPIE* **4612**, 128–135.
18. Moore, J. V., M. L. Waller, S. Zhao, N. J. Dodd, P. D. Acton, A. P. Jeavons and D. L. Hastings (1998) Feasibility of imaging photodynamic injury to tumours by high-resolution positron emission tomography. *Eur. J. Nucl. Med.* **25**, 1248–1254.
19. Molckovsky, A. and B. C. Wilson (2001) Monitoring of cell and tissue responses to photodynamic therapy by electrical impedance spectroscopy. *Phys. Med. Biol.* **46**, 983–1002.
20. Gersing, E., D. K. Kelleher and P. Vaupel (2003) Tumour tissue monitoring during photodynamic and hyperthermic treatment using bioimpedance spectroscopy. *Physiol. Meas.* **24**, 625–637.
21. Wang, I., S. Andersson-Engels, G. E. Nilsson, K. Wardell and K. Svanberg (1997) Superficial blood flow following photodynamic therapy of malignant non-melanoma skin tumours measured by laser Doppler perfusion imaging. *Br. J. Dermatol.* **136**, 184–189.
22. Jacques, S. L., J. A. Viator and G. Paltauf (2000) Optoacoustic imaging of tissue blanching during photodynamic therapy of esophageal cancer. *Proc. SPIE* **3916**, 322–330.
23. Chen, Z., T. E. Milner, X. Wang, S. Srinivas and J. S. Nelson (1998) Optical Doppler tomography, imaging in vivo blood flow dynamics following pharmacological intervention and photodynamic therapy. *Photochem. Photobiol.* **67**, 56–60.
24. Yang, V. X. D., M. L. Gordon, B. Qi, E. S. Yue, S. Tang, S. Bisland, J. Pekar, S. Lo, N. Marcon, B. C. Wilson and I. A. Vitkin (2003) High sensitivity detection and monitoring of microcirculation using cutaneous and catheter probes for Doppler optical coherence tomography. *Proc. SPIE* **4965**, 153–159.
25. Wilson, B. C., R. A. Weersink and L. Lilge (2003) Fluorescence in photodynamic therapy dosimetry. In *Handbook of Biomedical Fluorescence* (Edited by M. A. Mycek and B. W. Pogue), pp. 529–561. Marcel Dekker Inc., New York.
26. Zeng, H., M. Korbelik, D. I. McLean, C. MacAulay and H. Lui (2002) Monitoring photoproduct formation and photobleaching by fluorescence spectroscopy has the potential to improve PDT dosimetry with a verteporfin-like photosensitizer. *Photochem. Photobiol.* **75**, 398–405.
27. Contag, P. R., I. N. Olomu, D. K. Stevenson and C. H. Contag (1998) Bioluminescent indicators in living mammals. *Nat. Med.* **4**, 245–247.
28. Contag, C. H., D. Jenkins, P. R. Contag and R. S. Negrin (2000) Use of reporter genes for optical measurements of neoplastic disease in vivo. *Neoplasia* **2**, 41–52.
29. Zhang, L., K. E. Hellstrom and L. Chen (1994) Luciferase activity as a marker of tumor burden and as an indicator of tumor response to antineoplastic therapy in vivo. *Clin. Exp. Metastasis* **12**, 87–92.
30. Rice, B. W., M. D. Cable and M. B. Nelson (2001) In vivo imaging of light-emitting probes. *J. Biomed. Opt.* **6**, 432–440.
31. Hilali, N., N. Rubio, M. Martinez-Villacampa and J. Blanco (2002) Combined noninvasive imaging and luminometric quantification of luciferase-labeled human prostate tumors and metastases. *Lab. Invest.* **82**, 1563–1571.
32. Contag, C. H. and B. D. Ross (2002) It's not just about anatomy: in vivo bioluminescence imaging as an eyepiece into biology. *J. Magn. Reson. Imaging* **16**, 378–387.
33. Rehemtulla, A., L. D. Stegman, S. J. Cardozo, S. Gupta, D. E. Hall, C. H. Contag and B. D. Ross (2000) Rapid and quantitative assessment of cancer treatment response using in vivo bioluminescence imaging. *Neoplasia* **2**, 491–495.
34. Negrin, R. S., M. Edinger, M. Verneris, Y. A. Cao, M. Bachmann and C. H. Contag (2002) Visualization of tumor growth and response to NK-T cell based immunotherapy using bioluminescence. *Ann. Hematol.* **81**, 44–45.
35. Edinger, M., Y. A. Cao, M. R. Verneris, M. H. Bachmann, C. H. Contag and R. S. Negrin (2003) Revealing lymphoma growth and the efficacy of immune cell therapies using in vivo bioluminescence imaging. *Blood* **101**, 640–648.
36. Schlosser, V., O. R. Koechli, R. Cattaneo, B. Jentsch, U. Haller and H. Walt (1999) Photodynamic effects in vitro in fresh gynecologic tumors analyzed with a bioluminescence method. *Clin. Chem. Lab. Med.* **37**, 115–120.
37. Hamblin, M. R., D. A. O'Donnell, N. Murthy, C. H. Contag and T. Hasan (2002) Rapid control of wound infections by targeted photodynamic therapy monitored by in vivo bioluminescence imaging. *Photochem. Photobiol.* **75**, 51–57.
38. Hamblin, M. R., T. Zahra, C. H. Contag, A. T. McManus and T. Hasan (2003) Optical monitoring and treatment of potentially lethal wound infections in vivo. *J. Infect. Dis.* **187**, 1717–1725.
39. Chopp, M., M. O. Dereski, L. Madigan, F. Jiang and B. Logie (1996) Sensitivity of 9L gliosarcomas to photodynamic therapy. *Radiat. Res.* **146**, 461–465.
40. Shevchuk, I., V. Chekulayev, J. Moan and K. Berg (1996) Effects of the inhibitors of energy metabolism, lonidamine and levamisole, on 5-aminolevulinic-acid-induced photochemotherapy. *Int. J. Cancer* **67**, 791–799.
41. Lilge, L., K. Menzies, S. Bisland, A. Lin and B. C. Wilson (2002) PDT induced apoptosis: investigations using two malignant brain tumor models. *Proc. SPIE* **4612**, 136–142.
42. Gibson, S. L., M. L. Nguyen, J. J. Havens, A. Barbarin and R. Hilf (1999) Relationship of delta-aminolevulinic acid-induced protoporphyrin IX levels to mitochondrial content in neoplastic cells in vitro. *Biochem. Biophys. Res. Commun.* **265**, 315–321.
43. Tsujimoto, Y. (1997) Apoptosis and necrosis: Intracellular ATP level as a determinant for cell death modes. *Cell Death Differ* **4**, 429–424.
44. Lilge, L., M. Portnoy and B. C. Wilson (2000) Apoptosis induced in vivo by photodynamic therapy in normal brain and intracranial tumour tissue. *Br. J. Cancer* **83**, 1110–1117.
45. Sherf, B. A. and K. Y. Wood (1994) Firefly luciferase engineered to improve genetic reporting. *Promega Notes* **49**, 14–24.
46. Omiya, Y., T. Hirano and M. Ohashi (1996) The structural origin of the color differences in the bioluminescence of firefly luciferase. *FEBS Lett.* **384**, 83–86.
47. Chen, Q., Z. Huang, D. Luck, J. Beckers, P. H. Brun, B. C. Wilson, A. Scherz, Y. Salomon and F. W. Hetzel (2002) Preclinical studies in normal canine prostate of a novel palladium-bacteriopheophorbide (WSR09) photosensitizer for photodynamic therapy of prostate cancers. *Photochem. Photobiol.* **76**, 438–445.
48. Granville, D. J., J. G. Levy and D. W. Hunt (1997) Photodynamic therapy induces caspase-3 activation in HL-60 cells. *Cell Death Differ.* **4**, 623–628.
49. Hanlon, J. G., K. Adams, A. J. Rainbow, R. S. Gupta and G. Singh (2001) Induction of Hsp60 by Photofrin-mediated photodynamic therapy. *J. Photochem. Photobiol. B: Biol.* **64**, 55–61.
50. Wang, H. P., J. G. Hanlon, A. J. Rainbow, M. Espiritu and G. Singh (2002) Up-regulation of Hsp27 plays a role in the resistance of human

colon carcinoma HT29 cells to photooxidative stress. *Photochem. Photobiol.* **76**, 98–104.
51. Mitra, S., E. M. Goren, J. G. Frelinger and T. H. Foster (2003) Activation of heat shock protein 70 promoter with meso-tetrahydroxyphenyl chlorin photodynamic therapy reported by green fluorescent protein in vitro and in vivo. *Photochem. Photobiol.* **78**, 615–622.
52. Shibata, T., N. Akiyama, M. Noda, K. Sasai and M. Hiraoka (1998) Enhancement of gene expression under hypoxic conditions using fragments of the human vascular endothelial growth factor and the erythropoietin genes. *Int. J. Radiat. Oncol. Biol. Phys.* **42**, 913–916.
53. Ferrario, A., K. F. von Tiehl, N. Rucker, M. A. Schwarz, P. S. Gill and C. J. Gomer (2000) Antiangiogenic treatment enhances photodynamic therapy responsiveness in a mouse mammary carcinoma. *Cancer Res.* **60**, 4066–4069.
54. Wang, G. L. and G. L. Semenza (1995) Purification and characterization of hypoxia-inducible factor 1. *J. Biol. Chem.* **270**, 1230–1237.
55. Bogaards, A., A. Varma, E. H. Moriyama, A. Lin, A. Giles, S. Bisland, L. Lilge, G. M. Bilbao, P. J. Muller and B. C. Wilson (2003) Fluorescence-guided resection of intracranial VX2 tumor in a preclinical model using 5-aminolevulinic acid (ALA), preliminary results. *Proc. SPIE* **4952**, 91–96.
56. Stummer, W., A. Novotny, H. Stepp, C. Goetz, K. Bise and H. J. Reulen (2000) Fluorescence-guided resection of glioblastoma multiforme by using 5-aminolevulinic acid-induced porphyrins, a prospective study in 52 consecutive patients. *J. Neurosurg.* **93**, 1003–1013.
57. Shinoda, J., H. Yano, S. Yoshimura, A. Okumura, I. Kaku and N. S. Sakai (2003) Fluorescence-guided resection of glioblastoma multiforme by using high-dose fluorescein sodium. *J. Neurosurg.* **99**, 597–603.
58. Yang, V. X., P. J. Muller, P. Herman and B. C. Wilson (2003) A multispectral fluorescence imaging system, design and initial clinical tests in intra-operative Photofrin-photodynamic therapy of brain tumors. *Lasers Surg. Med.* **32**, 224–232.